ChemComm

Accepted Manuscript

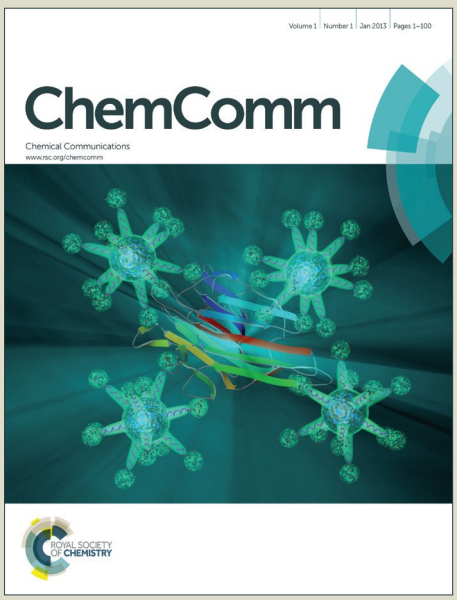

ROYAL SOCIETY OF CHEMISTRY

www.rsc.org/chemcomm

ChemComm

RSCPublishing

COMMUNICATION

The Facile Realization of RGB Luminescence based on One Yellow Emissive Four-Coordinate Organoboron Material

Cite this: DOI: 10.1039/x0xx00000x

Received 00th January 2012,
Accepted 00th January 2012

DOI: 10.1039/x0xx00000x

www.rsc.org/

Lu Wang,[a] Kai Wang[b], Houyu Zhang[a], Chuanjun Jiao[a], Bo Zou[b]*, Kaiqi Ye[a], Hongyu Zhang[a]* and Yue Wang[a]

The orange emissive powders of a boron-containing compound generate red, green, and blue luminescence after compressing, heating, and volatile acid fuming, respectively. Thus, stimulus-induced RGB emissions have been facilely realized based on one organic π–conjugated material for the first time, to the best of our knowledge.

Organic π–conjugated emitters have recently attracted much attention owing to their wide applications in organic light-emitting diodes (OLEDs), organic solid-state lasers (OSLs), and fluorescent sensors.[1,2] Red (**R**), green (**G**) and blue (**B**) are primary emissions which can generate other visible lights such as yellow, pink, white and so on by the suitable combination of them. Thus, the development of **RGB** luminescent materials is one of the prerequisites for realizing full-color optoelectronic applications. Various design strategies and structural modifications have been employed to construct organic materials with intense **RGB** luminescence. Due to the huge energy difference, the basic structures of **RGB** emitters are generally different. Non-conjugated or nonpolar structures are usually adopted to synthesize blue emissive compounds whereas extended π-conjugation or strong polarity is mostly chosen for designing red fluorescent molecules. Therefore, the realization of **RGB** luminescence requires complex molecular design as well as laborious synthetic work.

The luminescence of organic π–conjugated materials depends on not only the nature of constituent molecules but also the aggregation mode of collective ones.[3] Thus, molecular conformation and/or packing manners significantly affect the luminescence of solid samples and multicolor emissions based on one compound may be achieved by properly environmental induction.[4] For instance, some organic solids display varied luminescence after physical treating like grinding[5], heating[6], irradiating[7] and volatile organic solvent fuming[8]. However, most examples reported so far have shown the spectrum shift less than 50 nm which is much smaller than the difference (ca. 80 nm) between neighboring primary colors (**B**/**G** and **G**/**R**). Although **BG** or **GR** emissions have been recently achieved through either chemical or physical treatment[9], one-molecule based materials that can produce **RGB** emissions by environmental modification have not yet been found. Cyan (ca. 490 nm) and orange (ca. 590 nm) luminescence locate at the middle between **B**/**G** and **G**/**R**, respectively. Hence materials with either one of the two emissions may produce **BG** or **GR** emissions through molecular conformation/packing modulation. However, the realization of the third one (**R** or **B**) requires the spectral shifts over 100 nm which is hard to realize by conformation/packing modification. Recent results indicate that huge spectral shift over 100 nm can be achieved by enhancing or weakening intramolecular charge-transfer (ICT) strength of donor (D)-acceptor (A) type organic materials.[10] In this sense, D-A structured organic materials with appropriate fluorescence are possible candidates to generate **RGB** emissions by external induction (orange: route **a**; cyan: route **b**) if their structures are ideally furnished (Chart 1). To achieve this goal, we employ a boron-containing molecule **1** (Scheme S1) by considering the following aspects: (a) the molecular structure composes donor and acceptor moieties with ICT strength-dependent fluorescence; (b) the material has polymorphic nature with phase-dependent emissions and (c) the solids display luminescence locating at the middle of two primary emissions **G** and **R**. The facilely realization of **RGB** luminescence based on this boron-containing solids (route **a**) has been elucidated in detail.

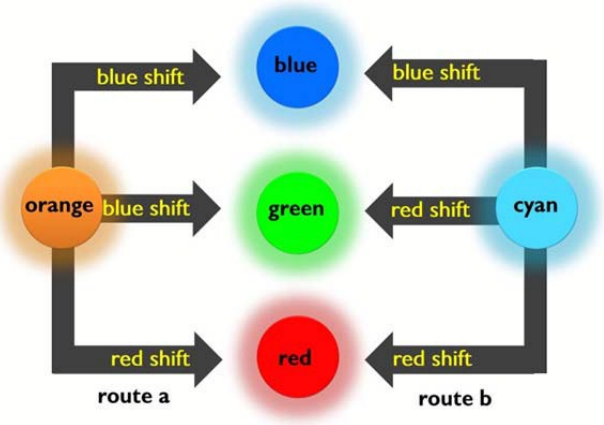

Chart 1 Possible routes of stimuli-induced **RGB** luminescence based on one organic compound.

The emission behaviours of compound **1** have not been deeply investigated although it is a known molecule.[11] In this work, molecule **1** was synthesized by refluxing the mixture of 1,3-diaryl-*β*-diketone and fluorobis(pentafluorophenyl)borane in THF overnight. Recrystallization of the reaction mixture gives rise to orange crystalline powders which display typical solvent-dependent luminescence, namely, the emission spectrum red-shifts upon increasing the polarity of solvent (Fig. S1). The highest occupied molecular orbital (HOMO) and the lowest unoccupied molecular orbital (LUMO) are separately localized on aniline group and diketonate moiety, respectively. Time-dependent density functional theory calculations indicate the vertical transition is mainly originated from HOMO to LUMO, demonstrating the fluorescence of **1** has strong ICT character (Fig. S2).

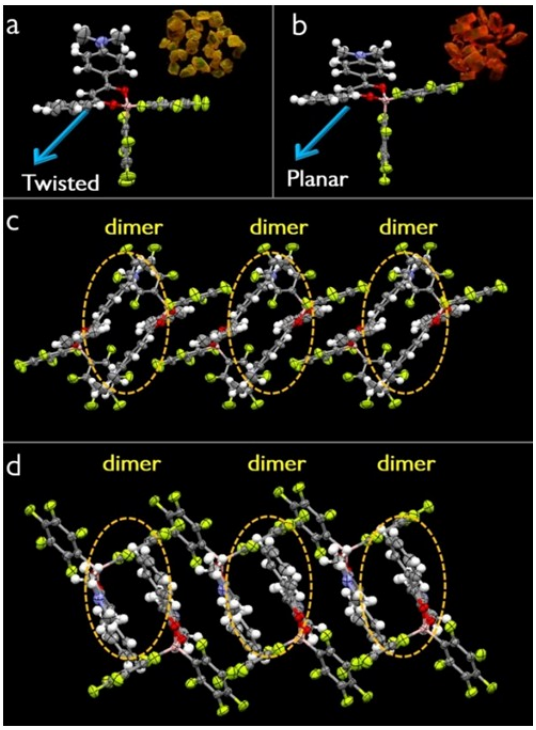

Fig. 1 Molecular conformations (a, b) and packing structures (c, d) of polymorphs **1OC** and **1RC** (a and c for **1OC** and b and d for **1RC**; inset: photographic images of **1OC** and **1RC** under UV irradiation).

High-quality orange crystals (**1OC**) with emission peak (λ_{em}) at about 580 nm and quantum yield (Φ_F) of 0.33 can be easily obtained by either solvent diffusion or vacuum sublimation approaches. Noteworthy is that small amount of red crystals (**1RC**, λ_{em} = 615 nm; Φ_F = 0.43) are found in orange ones (Fig. S3). **1OC** and **1RC** which are orange and red emissive, respectively, can be easily identified and separated owing to their obviously different colors and emissions (Fig. 1). **1RC** crystals have longer lifetime (5.67 ns) than **1OC** sample (1.61 ns) does. To reveal the essence of luminescent difference, crystals **1OC** and **1RC** are tested through X-ray diffraction. Both crystals hold the same crystal system (triclinic) and space group (*P*-1) and the unit cells contain only one individual molecule. Boron atoms adopt typical four-coordinate geometry and the bond lengths and angles are comparable (Fig. S4). Interestingly, the molecular conformations are quite different in the ligand part (Fig. 1a and b). The dihedron angles between aniline and phenyl rings are 30° for **1OC** and 18° for **1RC**, indicating that the ligand of **1OC** is more distorted than that of **1RC**. The HOMO and LUMO orbitals seem quite similar in these two conformations, but the HOMO–LUMO gap of **1RC** is smaller than that of **1OC** due to the more planar structures (Figs. S5 and 6). The calculated absorption spectrum of **1RC** is red-shifted by 7.3 nm compared with that of **1OC**, which is consistent with the HOMO–LUMO gaps. As shown in Fig. 1c and d, the adjacent two molecules in both crystals are π–stacked into dimers (π–π distance: 3.4 Å for **1OC** and 3.5 Å for **1RC**), which further pack into column structures with different arrangements. The calculated transition dipole moments in the crystal states are similar, being 13.63 Debye for **1OC** and 13.54 Debye for **1RC** (Fig. S7). Therefore, the absorption and emission properties in our investigated system not only depend on the intrinsic electronic nature of single molecule itself, but also rely on the relative molecular orientations and intermolecular interactions. This boron compound presents a model of organic π–conjugated materials with polymorph-dependent luminescence.

The luminescence of **1OC** displays distinct response towards mechanical grinding and hydrostatic pressures. As shown in Fig. S8, the orange crystals **1OC** readily convert into orange red solids **1OR** after simple mechanically grinding accompanied with the emission peak shifting from 580 nm to 610 nm ($\Delta\lambda_{em} \approx 30$ nm). The ground amorphous sample partially converts to crystalline solids when it is fumed by CH_2Cl_2 vapor in a closed container. Powder X-ray diffraction (PXRD) measurements are employed to disclose the changes of molecular arrangements during the mechanically grinding and solvent fuming cycle (Fig. S9). The unground sample **1O** shows intense and sharp diffraction peaks while the ground red

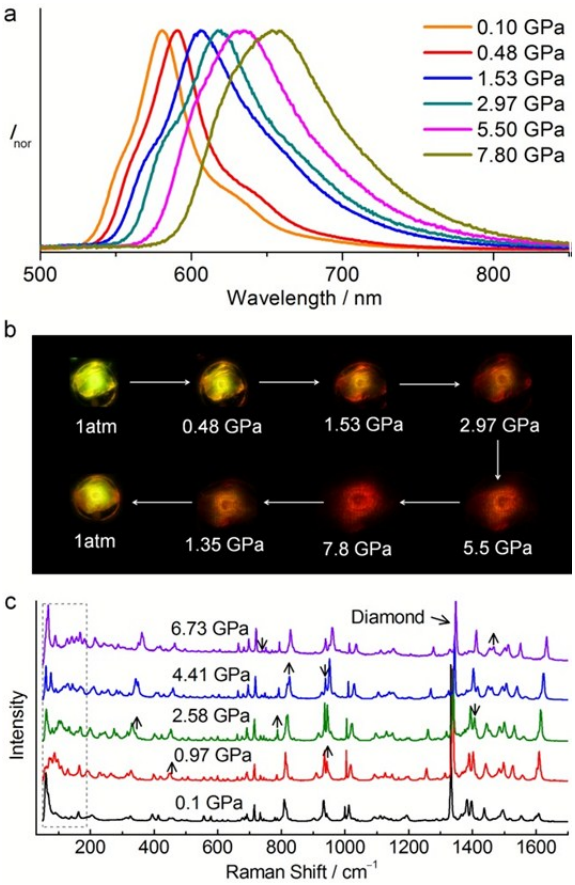

Fig. 2 (a) The luminescent spectra, (b) micrographs of the crystal **1OC** under different pressures and (c) high pressure Raman spectra.

solids display significantly weakened and broadened signals. This finding indicates the well-ordered molecular aggregates are deformed into a disordered structure. Different molecular arrangements induced by mechanical grinding might be responsible for the luminescent chromism. Indeed, the ground sample displays a different exothermic peak at about 90 °C in the DSC profile compared with **1OC** crystals (Fig. S10). After fumed by CH_2Cl_2, the intensity of PXRD pattern partially recover, which indicates the molecules repack into the initial ordered arrangement.

On the other hand, the luminescence of **1OC** solids significantly red shift under certain hydrostatic pressure performed by using a diamond anvil cell. Fig. 2 shows the luminescence changes of the sample in the compressing and decompressing procedures. The luminescence of **1OC** gradually shifts to longer wavelength region upon increasing the hydrostatic pressure in the media of silicone oil. Deep red solid (**1R**) is obtained when the pressure approaches 7.8 GPa and the emission maximum (655 nm) red shift by about 75 nm compared with the uncompressed sample (580 nm). Both color and emission recover when decompressing the sample under atmospheric pressure (Fig. S12. To understand the detailed pressure-induced structural variation, we have performed *in situ* high pressure Raman measurements (Fig. 2c). It seems that the external modes (below 200 cm^{-1}) exhibit substantial change and blue shift under pressure, which is due to the change of intermolecular distances. Raman peaks in this internal modes region (200–1700 cm^{-1}) also shift gradually toward higher frequencies. As the crystal is compressed, the increases in frequencies can be explained by the decrease of interatomic distances and the increase in the effective force constants. Apart from a continuous shift to higher frequencies, many Raman peaks also show changes of the relative intensity. The increase or decrease of relative intensity can be attributed to the pressure-induced molecular conformation alterations and ligand distortion. After the pressure is released, the Raman spectrum is found to be the same as what it was before pressure was applied, indicating that the compression is reversible.

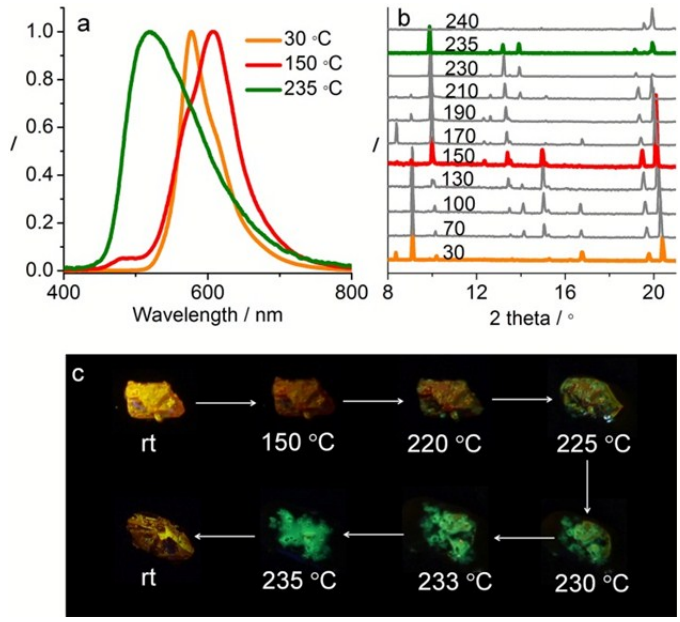

Fig. 3 (a) Emission spectra at 50 °C, 150 °C and 235 °C, (b) temperature-dependent PXRD curves and (c) photographic images of **1OC** sample in the heating and cooling process.

In addition, the sample **1OC** shows interesting thermochromic behaviors (Fig. 3). Upon slowly increasing temperature to 150° C, the fluorescence of the sample red-shifts from 580 nm to 610 nm. A novel emission band peaking around 520 nm appears and intensity of the previous band gradually decreases when we further increase the temperature (Fig. S13). Finally, the orange sample **1OC** totally transfers into a green emissive solid (**1G**) at about 235 °C which is slightly lower than its melting point (245 °C), as shown in Fig. 3c. The luminescence of the heated sample **1G** blue-shift by 60 nm compared with that of **1OC**. The heating-induced green luminescence can only survive under high temperature. Both color and luminescence of the heated sample recover when the temperature falls below 150 °C. Crystal deformation takes place at high temperature based on the photographic images shown in Fig. 3c. To get insights into this interesting heating-induced luminescence change, we have carried out temperature-dependent PXRD and DSC measurements which can give molecular packing information of the sample during the heating process in real-time. At room temperature, the crystalline sample shows intense and sharp diffraction peaks which keep almost unchanged when the temperature is below 150 °C. Novel PXRD signals appears when the temperature is over 150 °C and some diffraction peaks disappear at the same time, indicating that molecular repacking takes place at a high temperature. The DSC profile (Fig. S10) of **1OC** crystals show weak and broad peaks at about 130 and 220 °C, further confirming that phase transitions occur during the heating process. Although the mechanism of this thermochromism cannot be clearly proposed at the current stage, we assume that the closely approached molecules have been taken apart under high temperature and the sample displays the luminescence of the individual molecule.

Gao and co-workers have reported the fluorescent sensing behaviour of the present compound toward hydrochloric acid (HCl) gas.[11] They found that a TLC plate containing this boron material showed dramatically luminescent change when exposed to HCl gas. Interestingly, **1OC** crystals exhibit acidochromic behaviour with self-healing properties. Accompanied with the dramatically fluorescence change from 580 nm to 450 nm, the sample **1OC** deforms into sticky colorless solid **1B** after fumed with strong volatile acid such as hydrochloric acid (HCl) or trifluoroacetic acid (TFA). Thus, blue luminescence has been achieved through stimulating the orange emissive solid. The acidified sample can recover its original color and luminescence at ambient conditions, indicative of a self-healing property.

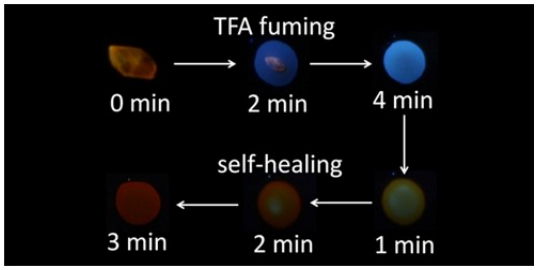

Fig. 4 Photographic images of the orange emissive sample before and after protonation.

Conclusions

In summary, we have reported the conformation-dependent emission behaviors of an organoboron material **1**. The fluorescence of **1** can be significantly affected by not only solvent polarity but also ICT strength. Owing to these intriguing emission behaviors, the solid-state luminescence of

this material can be easily modified by external stimuli like pressure, heat, and acid based on different mechanisms. Since the intrinsic orange luminescence locates at the proper position between green and red, ligand planarity or packing mode alternations of the orange fluorescent sample **1O** induced by physical approaches, which allows the production of green (**1G**) and red (**1R**) luminescence. Protonation of the donor section diminishes the ICT strength greatly, and hence shifts the orange emission to blue (**1B**) luminescence. Thus, **RGB** luminescence has been achieved based on one yellow emissive material. The present study not only provides a model of the facile realization of **RGB** luminescence based on one compound by external stimulation, but also gives design guidance towards smart luminescent organic materials.

Acknowledgements

This work was supported by the National Natural Science Foundation of China (51173067, 91333201 and 91227202), China Postdoctoral Science Foundation (No. 2012M511327) and Program for Chang Jiang Scholars and Innovative Research Team in University (No. IRT101713018).

Notes and references

[a] State Key Laboratory of Supramolecular Structure and Materials, College of Chemistry, Jilin University, Changchun 130012, P. R. China. hongyuzhang@jlu.edu.cn

[b] State Key Laboratory of Superhard Materials, Jilin University, Changchun 130012, P. R. China. zoubo@jlu.edu.cn

Electronic Supplementary Information (ESI) available: General information, synthetic detail and NMR spectra of compound **1**, PXRD curves, and emission spectrum of crystal **1OC** crystal **1OC**, DSC curve of sample **1O** and crystal structures of **1OC** and **1RC** in CIF format. See DOI: 10.1039/c000000x/

1 Recent reviews: a) Z. M. Hudson, S. Wang, *Acc. Chem. Res.,* 2009, **42**, 1584; b) T. M. Figueira-Duarte, K. Müllen, *Chem. Rev.,* 2011, **111**, 7260; c) D. Li, H. Zhang, Y. Wang, *Chem. Soc. Rev*., 2013, **42**, 8416; d) Y. Hong, J. W. Y. Lam, B. Z. Tang, *Chem. Soc. Rev*., 2011, **40**, 5361; e) Z. Chi, X. Zhang, B. Xu, X. Zhou, C. Ma, Y. Zhang, S. Liu, J. Xu, *Chem. Soc. Rev.,* 2012, **41**, 3878.

2 a) Y. Kim, J. Bouffard, S. E. Kooi, T. M. Swager, *J. Am. Chem. Soc.,* 2005, **127**, 13726; b) A. Wakamiya, K. Mori, S. Yamaguchi, *Angew. Chem. Int. Ed.,* 2007, **46**, 4273; c) D. Li, H. Zhang, C. Wang, S. Huang, J. Guo, Y. Wang, *J. Mater. Chem.,* 2012, **22**, 4319; d) A. Steffen, M. G. Tay, A. S. Batsanov, J. A. K. Howard, A. Beeby, K. Q. Vuong, X.-Z Sun, M. W George, T. B. Marder, *Angew. Chem. Int. Ed.,* 2010, **49**, 2349; e) J. C. Collings, A. C. Parsons, L. Porrès, A. Beeby, A. S. Batsanov, J. A. K. Howard, D. P. Lydon, P. J. Low, I. J. S. Fairlamb, T. B. Marder, *Chem. Commun.,* 2005, 2666.

3 a) S. Varughese, *J. Mater. Chem. C,* 2014, **2**, 3499; b) T. Mutai, H. Tomoda, T. Ohkawa, Y. Yabe, K. Araki, *Angew. Chem. Int. Ed.,* 2008, **47**, 9522; c) D. Yan, D. G. Evans, *Mater. Horiz.,* 2014, **1**, 46; d) X. Cheng, Z. Zhang, H. Zhang, S. Han, K. Ye, L. Wang, H. Zhang, Y. Wang, *J. Mater. Chem. C,* 2014, **2**, 7385; e) X. Cheng, D. Li, Z. Zhang, H. Zhang, Y. Wang, *Org. Lett.,* 2014, **16**, 880; f) K. Wang, H. Zhang, S. Chen, G. Yang, J. Zhang, W. Tian, Z. Su, Y. Wang, *Adv. Mater.,* 2014, **26**, 6168.

4 a) J. Liang, Z. Chen, L. Xu, J. Wang, J. Yin, G.-A. Yu, Z-N. Chen, S. H. Liu, *J. Mater. Chem. C,* 2014, **2**, 2243; b) C. Yuan, S. Saito, C. Camacho, T. Kowalczyk, S. Irle, S. Yamaguchi, *Chem. Eur. J.,* 2014, **20**, 2193; c) Z. Ma, M. Teng, Z. Wang, S. Yang, X. Jia, *Angew. Chem. Int. Ed.,* 2013, **52**, 12268; d) T. Seki, K. Sakurada, H. Ito, *Angew. Chem. Int. Ed.,* 2013, **52**, 12828; e) X. Luo, J. Li, C. Li, L. Heng, Y. Q. Dong, Z. Liu, Z. Bo, B. Z. Tang, *Adv. Mater.,* 2011, **23**, 3261; f) D. Liu, Z. Zhang, H. Zhang, Y. Wang, *Chem. Commun.,* 2013, **49**, 10001.

5 a) M. Krikorian, S. Liu, T. M. Swager, *J. Am. Chem. Soc.,* 2014, **136**, 2952; b) Z.-H. Guo, Z.-X. Jin, J.-Y. Wang, J. Pei, *Chem. Commun.,* 2014, **50**, 6088.

6 a) X. Liu, S. Li, J. Feng, Y. Li, G. Yang, *Chem. Commun.,* 2014, **50**, 2778; b) X.-C. Shan, H.-B. Zhang, L. Chen, M.-Y. Wu, F.-L. Jiang, M.-C. Hong, *Cryst. Growth Des.,* 2013, **13**, 1377.

7 a) J. W. Chung, S.-J. Yoon, B.-K. An, S. Y. Park, *J. Phys. Chem. C,* 2013, **117**, 11285; b) K. M. Hutchins, S. Dutta, B. P. Loren, L. R. MacGillivray, *Chem. Mater.,* 2014, **26**, 3042; c) Z. Zhang, D. Yao, T. Zhou, H. Zhang, Y. Wang, *Chem. Commun.,* 2011, **47**, 7782.

8 a) E. Cariati, C. Dragonetti, E. Lucenti, F. Nisic, S. Righetto, D. Roberto, E. Tordin, *Chem. Commun.,* 2014, **50**, 1608; b) L. Shi, Y. Fu, C. He, D. Zhu, Y. Gao, Y. Wang, Q. He, H. Cao, J. Cheng, *Chem. Commun.,* 2014, **50**, 872; c) T. Han, X. Feng, J. Shi, B. Tong, Y. Dong, J. W. Y. Lam, Y. Dong, B. Z. Tang, *J. Mater. Chem. C,* 2013, **1**, 7534.

9 a) X. Y. Shen, Y. J. Wang, E. Zhao, W. Z. Yuan, Y. Liu, P. Lu, A. Qin, Y. Ma, J. Z. Sun, B. Z. Tang, *J. Phys. Chem. C,* 2013, **117**, 7334; b) K. Nagura, S. Saito, H. Yusa, H. Yamawaki, H. Fujihisa, H. Sato, Y. Shimoikeda, S. Yamaguchi, *J. Am. Chem. Soc.,* 2013, **135**, 10322; c) C. Li, X. Luo, W. Zhao, C. Li, Z. Liu, Z. Bo, Y. Dong, Y. Q. Dong, B. Z. Tang, *New. J. Chem.,* 2013, **37**, 1696; d) X. Luo, W. Zhao, J. Shi, C. Li, Z. Liu, Z. Bo, Y. Q. Dong, B. Z. Tang, *J. Phys. Chem. C,* 2012, **116**, 21967.

10 a) Y. Dong, J. Zhang, X. Tan, L. Wang, J. Chen, B. Li, L. Ye, B. Xu, B. Zou, W. Tian, *J. Mater. Chem. C,* 2013, **1**, 7554; b) Q. Qi, X. Fang, Y. Liu, P. Zhou, Y. Zhang, B. Yang, W. Tian, S. X.-A. Zhang, *RSC. Adv.,* 2013, **3**, 16986; c) H. Jeon, J. Lee, M. H. Kim, J. Yoon, *Macromol. Rapid. Commun.,* 2012, **33**, 972; d) K. Wang, S. Huang, Y. Zhang, S. Zhao, H. Zhang, Y. Wang, *Chem. Sci.,* 2013, **4**, 3288.

11 J. Hu, Z. He, Z. Wang, X. Li, J. You, G. Gao, *Tetrahedron Lett.,* 2013, **54**, 4167.

Journal Name RSCPublishing

COMMUNICATION

Graphical abstract

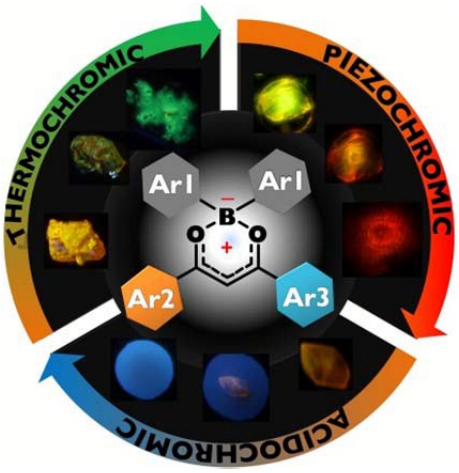

RGB luminescence has been achieved based on one yellow emissive four-coordinate boron-containing material by compressing, heating and acid fuming, respectively. The present study not only provides a model of the facile realization of RGB luminescence based on one compound by external stimulating approach but also give a design guidance towards smart luminescent organic materials.